

SUPPORTING INFORMATION

**Facile CO₂ Separation and Subsequent H₂ Production via Chemical-Looping Combustion
over Ceria-Zirconia Solid Solutions**

Kent J. Warren^a, Caroline M. Hill^a, Richard J. Carrillo^a, and Jonathan R. Scheffe^{a,*}

^a Department of Mechanical and Aerospace Engineering, University of Florida, Gainesville,
USA, 32611

* Corresponding author. Phone: +1 352-392-0839; Email Address: jscheffe@ufl.edu

S.1. Derivation of Redox Equilibrium Expression

According to the first and second laws of thermodynamics, at constant temperature (T) and pressure (P), the chemical equilibrium of a single or multi-reaction system is established when the following criterion is satisfied,

$$\sum_j v_j \mu_j = 0 \quad (\text{S.1})$$

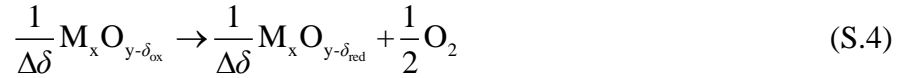
where v and μ refer to the stoichiometric coefficient and corresponding chemical potential (defined below in Equation S.2) of component j , respectively.^[1]

$$\mu_j \equiv \bar{G}_j(T, P) + RT \ln(y_j) \quad (\text{S.2})$$

Here, \bar{G} and y represent the molar Gibbs energy and mole fraction of each pure component in its physical state (*i.e.*, gas, liquid, or solid) within an ideal solution; the universal gas constant is denoted by R . More generally, thermodynamic activities are introduced to describe non-ideal or real mixtures and may be defined relative to standard states other than pure components.^[2] Thus, for convenience, Equation S.2 is rewritten to leverage the activity (a) and standard molar Gibbs energy (\bar{G}°) of component j , which is defined at fixed composition and ambient pressure (*i.e.*, 1 bar).

$$\mu_j \equiv \bar{G}_j^\circ(T, P^\circ) + RT \ln(a_j) \quad (\text{S.3})$$

Consider the following reduction reaction of a generic binary metal oxide (M_xO_y),



where δ_{red} and δ_{ox} are the oxygen nonstoichiometry at reduction and oxidation states, respectively. Chemical equilibrium of Equation S.4 may be mathematically described via substitution of Equation S.3 into Equation S.1; the result is shown below. Gaseous oxygen is assumed ideal, such that the fugacity coefficient is equal to unity, and thus the activity is replaced by partial pressure (p), as is typical.^[3] Recall that the standard molar Gibbs energy of O_2 is 0 kJ mol^{-1} .

$$\frac{1}{\Delta\delta} \left\{ \bar{G}_{M_x O_{y-\delta_{\text{red}}}}^\circ - \bar{G}_{M_x O_{y-\delta_{\text{ox}}}}^\circ \right\} = -RT \left\{ \frac{1}{\Delta\delta} \ln \left(\frac{a_{M_x O_{y-\delta_{\text{red}}}}}{a_{M_x O_{y-\delta_{\text{ox}}}}} \right) + \frac{1}{2} \ln \left(\frac{p_{O_2}}{P^\circ} \right) \right\} \quad (\text{S.5})$$

The difference in the Gibbs energies of products and reactants, weighted by their stoichiometric coefficients (*i.e.*, LHS of Equation S.5), will be expressed hereafter as $\Delta \bar{G}_{\text{red}}^\circ$ and is otherwise referred to the standard molar Gibbs energy change of Equation S.4. As noted by Cooper *et al.*, taking the limit for an infinitesimal change in oxygen nonstoichiometry (*i.e.*, $\Delta\delta \rightarrow 0$) yields the following expression for the standard partial molar Gibbs energy of oxygen vacancy formation ($\Delta \bar{g}_O^\circ$).^[4]

$$\Delta \bar{g}_{\text{O}}^{\circ}(\delta, T) \equiv \left[\frac{\partial (\Delta \bar{G}_{\text{red}}^{\circ})}{\partial \delta} \right]_{T, P, n_{\text{O}_2}(\text{g})} = \lim_{\Delta \delta \rightarrow 0} \Delta \bar{g}_{\text{red}}^{\circ} \quad (\text{S.6})$$

Partial properties are functions of composition, and in the limit that a solution becomes pure in species j , the partial and total properties (denoted here by lowercase and uppercase letters, respectively) approach. As a result, the RHS of Equation S.6 and LHS of Equation S.5 are mathematically equivalent.

$$\lim_{\Delta \delta \rightarrow 0} \Delta \bar{g}_{\text{red}}^{\circ} = \lim_{\Delta \delta \rightarrow 0} \Delta \bar{G}_{\text{red}}^{\circ} \quad (\text{S.7})$$

Furthermore, in this limit, the activities of the solid are uniform, and thus Equation S.5 may be simplified as follows.

$$\Delta \bar{g}_{\text{O}}^{\circ}(\delta, T) = -\frac{1}{2} RT \ln \left(\frac{p_{\text{O}_2}}{P^{\circ}} \right) \quad (\text{S.8})$$

Importantly, $\Delta \bar{g}_{\text{O}}^{\circ}$ can be additionally related to the standard partial molar enthalpy ($\Delta \bar{h}_{\text{O}}^{\circ}$) and entropy ($\Delta \bar{s}_{\text{O}}^{\circ}$) through differentiation with respect to temperature; the governing equation for chemical equilibrium of metal oxide reduction is shown below.

$$\Delta \bar{g}_{\text{O}}^{\circ}(\delta, T) = \Delta \bar{h}_{\text{O}}^{\circ}(\delta) - T \Delta \bar{s}_{\text{O}}^{\circ}(\delta) = -\frac{1}{2} RT \ln \left(\frac{p_{\text{O}_2}}{P^{\circ}} \right) \quad (\text{S.9})$$

Under the assumption that $\Delta \bar{h}_{\text{O}}^{\circ}$ and $\Delta \bar{s}_{\text{O}}^{\circ}$ are temperature-independent, these thermodynamic state functions can be determined from equilibrium δ versus p_{O_2} isotherms, without requiring explicit knowledge of defect chemistry, by evaluating the slope and intercept of generated van't Hoff plots at constant composition. This methodology has been previously adopted to extract compositionally-dependent, partial-molar properties of oxygen vacancy formation for ceria^[5] and ceria-zirconia solid solutions,^[6] thus enabling determination of equilibrium δ as a function of p_{O_2} and T . For this work, the digitized equilibrium data and concomitant partial properties for $\text{CeO}_{2-\delta}$ and $\text{Ce}_{1-x}\text{Zr}_x\text{O}_{2-\delta}$ ($x \leq 0.20$) can be observed in Figure S2. It should be noted that although equilibrium yields were evaluated slightly outside of the experimentally considered temperature ranges, the strong linear dependence observed in van't Hoff plots suggests that the assumption of temperature independence on $\Delta \bar{h}_{\text{O}}^{\circ}$ and $\Delta \bar{s}_{\text{O}}^{\circ}$ is valid.

S.2. Supporting Figures

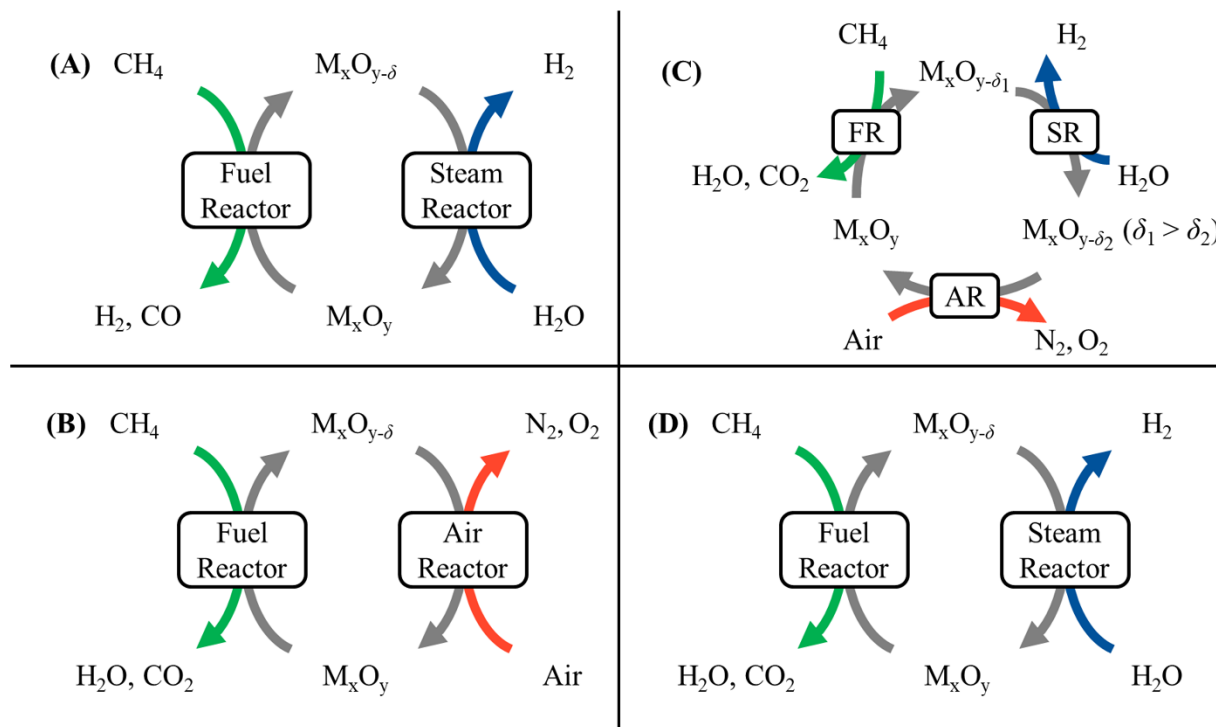


Figure S1. Compilation of chemical-looping techniques that leverage the oxygen-exchange capacity of metal oxides, denoted as M_xO_y , to produce fuel and/or sequester CO_2 . (A) Chemical-looping reforming, CLR. (B) Conventional chemical-looping combustion, CLC. (C) Three-reactor chemical-looping hydrogen generation, TRCL. (D) Two-reactor chemical-looping hydrogen generation, CLH (also referred to herein as CLC). In each process, CO_2 can replace H_2O as the steam reactor oxidant to generate pure streams of CO .

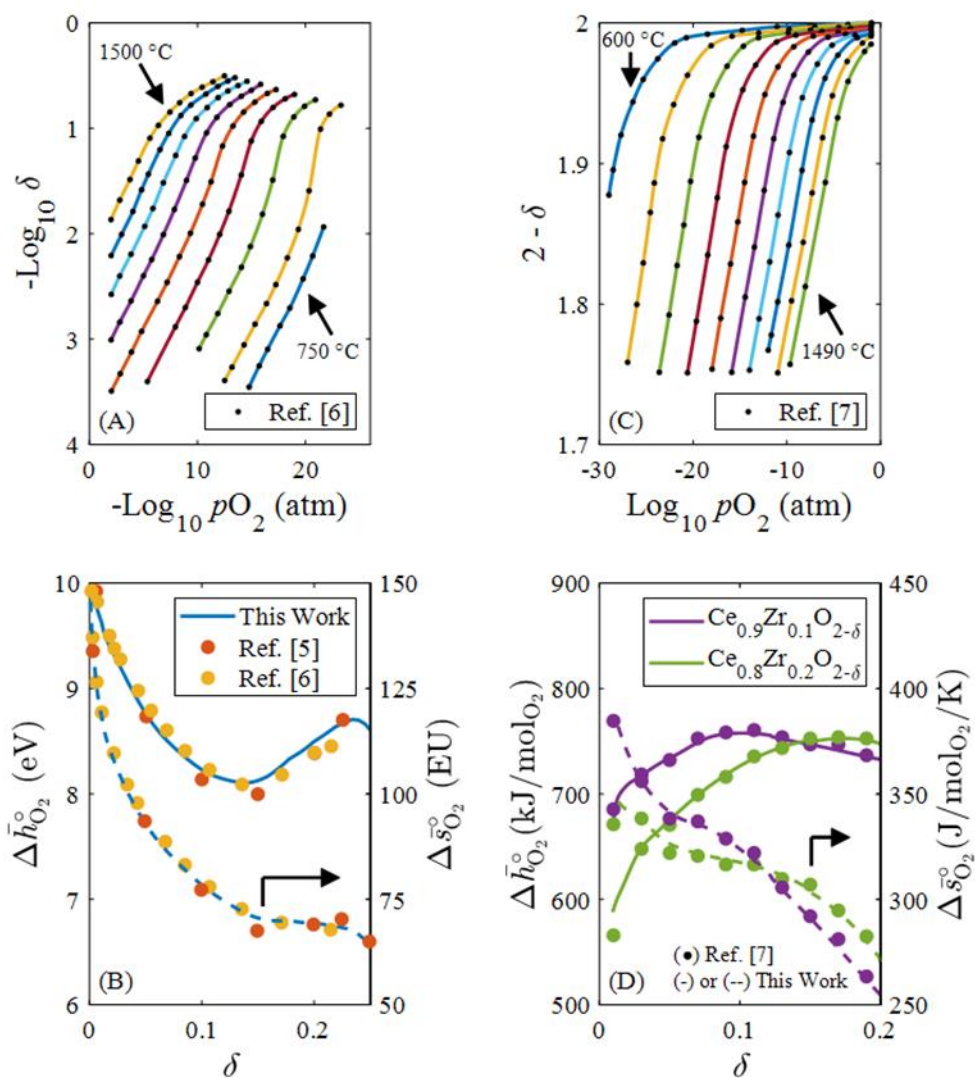


Figure S2. Extraction of standard partial molar properties for the reduction of $\text{CeO}_{2-\delta}$ (left panels) and $\text{Ce}_{1-x}\text{Zr}_x\text{O}_{2-\delta}$ (right panels) from previous works. Equilibrium δ versus $p\text{O}_2$ isotherms were digitized and are shown for (A) $\text{CeO}_{2-\delta}$ and (C) $\text{Ce}_{0.9}\text{Zr}_{0.1}\text{O}_{2-\delta}$. Following the van't Hoff methodology discussed in Section S.1, $\Delta\bar{h}_{\text{O}_2}^\circ$ (solid lines) and $\Delta\bar{s}_{\text{O}_2}^\circ$ (dashed lines) of considered oxides were determined as a function of δ and compared to representative literature, as shown in subplots (B) and (D). Here, $\Delta\bar{h}_{\text{O}_2}^\circ$ and $\Delta\bar{s}_{\text{O}_2}^\circ$ are equal to $2\Delta\bar{h}_{\text{O}}^\circ$ and $2\Delta\bar{s}_{\text{O}}^\circ$, respectively ($96.48 \text{ kJ mol}^{-1} = 1 \text{ eV}$ and $4.184 \text{ J mol}^{-1} \text{ K}^{-1} = 1 \text{ EU}$).

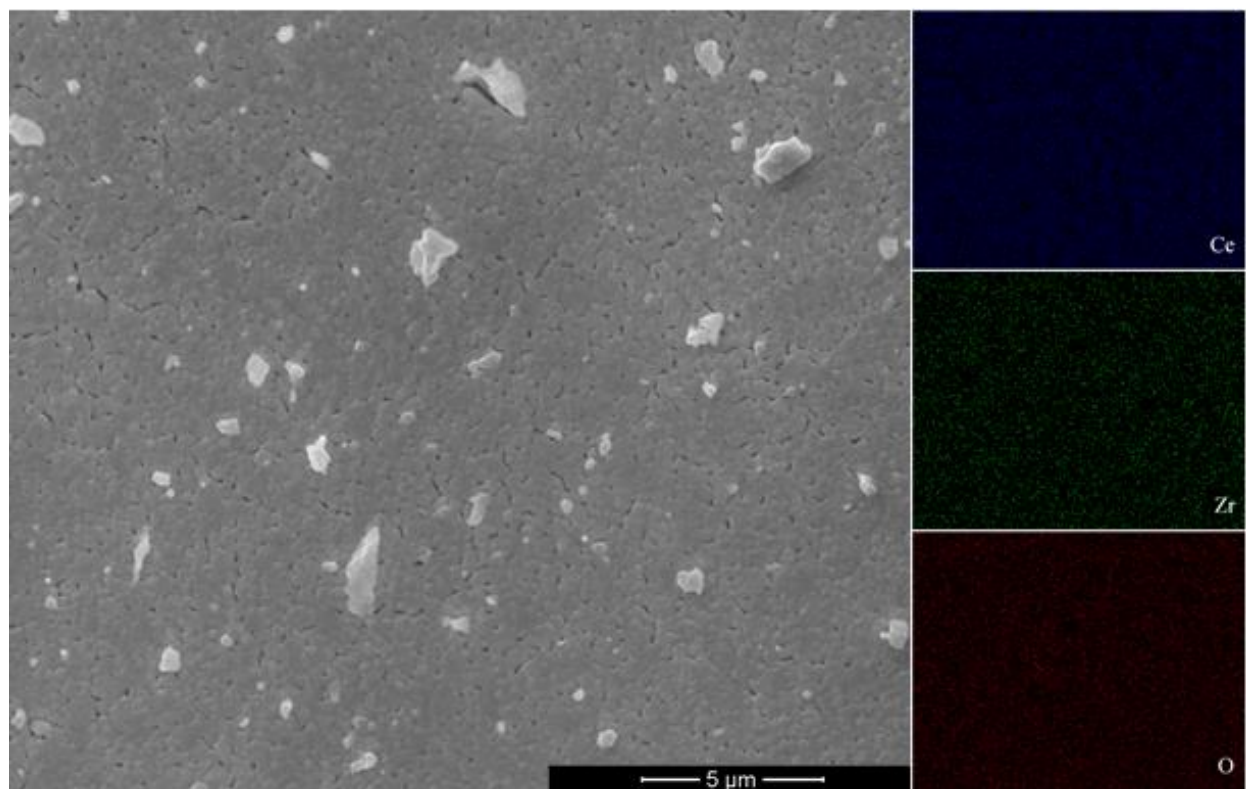


Figure S3. Representative scanning electron microscopy, SEM (left panel), and energy-dispersive X-ray spectroscopy, EDS (right panels), images of the $\text{Ce}_{0.9}\text{Zr}_{0.1}\text{O}_2$ powder used for thermogravimetric measurements. The position-dependent distributions of Ce, Zr, and O elements in $\text{Ce}_{0.9}\text{Zr}_{0.1}\text{O}_2$ are indicated by their respective colors in each EDS map.

References for Supporting Information

- [1] M. M. Abbott, J. M. Smith, H. C. Van Ness, *Introduction to Chemical Engineering Thermodynamics*, McGraw-Hill, **2005**.
- [2] J. D. Ramshaw, *Journal of chemical education* **1995**, *72*, 601.
- [3] S. Li, V. M. Wheeler, P. B. Kreider, W. Lipiński, *Energy Fuels* **2018**, *32*, 10838–10847.
- [4] T. Cooper, J. R. Scheffe, M. E. Galvez, R. Jacot, G. Patzke, A. Steinfeld, *Energy Technology* **2015**, *3*, 1130-1142.
- [5] a) D. Bevan, J. Kordis, *Journal of Inorganic and Nuclear Chemistry* **1964**, *26*, 1509-1523; b) R. Panlener, R. Blumenthal, J. Garnier, *Journal of Physics and Chemistry of Solids* **1975**, *36*, 1213-1222.
- [6] Y. Hao, C.-K. Yang, S. M. Haile, *Chemistry of Materials* **2014**, *26*, 6073-6082.